CMS Physics Analysis Summary

Contact: cms-pag-conveners-top@cern.ch 2012/07/14

Top pair cross section in e/mu+jets at 8 TeV

The CMS Collaboration

Abstract

A measurement is presented of the top quark pair-production cross section in $\sqrt{s} = 8$ TeV proton-proton collisions using data corresponding to an integrated luminosity of up to 2.8 fb^{-1}, collected by the CMS detector at the Large Hadron Collider. The analysis is performed in the top quark pair decay channel with one isolated, high transverse momentum electron or muon, and at least four hadronic jets. At least one jet is required to originate from a b-quark. The measured inclusive $\mathrm{t\bar{t}}$ cross section is: $\sigma_{\mathrm{t\bar{t}}} = 228.4 \pm 9.0\ (\mathrm{stat.})^{+29.0}_{-26.0}\ (\mathrm{syst.}) \pm 10.0\ (\mathrm{lum.})$ pb, in agreement with QCD predictions up to approximate next-to-next-to-leading order.

1 Introduction

Top quarks are abundantly produced at the Large Hadron Collider (LHC) [1], where the predicted next-to-leading order (NLO) cross section for top quark pair-production ($\sigma_{t\bar{t}}$) in proton-proton (pp) collisions, at the center-of-mass energy $\sqrt{s} = 8\,\text{TeV}$, is of the order of 225 pb [2]. A precise measurement of $\sigma_{t\bar{t}}$ is an important test of perturbative QCD at high energies. Furthermore, new physics processes can manifest themselves as an enhancement of the $t\bar{t}$ production rate.

The top quark pair-production cross section in the channel with one high-momentum lepton (electron or muon) and jets was measured at the LHC at $\sqrt{s} = 7\,\text{TeV}$ [3–5]. Here, a first measurement of the $t\bar{t}$ production cross section at $\sqrt{s} = 8\,\text{TeV}$ is presented using a dataset corresponding to an integrated luminosity of up to 2.8 fb^{-1} recorded by the Compact Muon Solenoid (CMS) experiment at the LHC.

In the standard model, top quarks are predominantly produced in pairs ($t\bar{t}$) via the strong interaction, and decay almost exclusively to a W boson and a bottom quark (b). The event signature is determined by the subsequent decays of the two W bosons. In this analysis we examine $t\bar{t}$ semileptonic decays into electrons or muons, *i.e.* the final state in which one of the W boson decays to $q'\bar{q}$ and the other to a charged lepton (electron or muon) and a neutrino. W boson decays into tau leptons are not specifically selected. The top quark decaying into the fully hadronic final state is referred to in the following as "hadronic top", while the top quark decaying leptonically is defined as "leptonic top". As two of the four jets result from the hadronization of the b and $\bar{b}$ quarks (b-jets), we employ b-tag algorithms for the identification of b-jets in order to improve the purity of our $t\bar{t}$ candidate sample.

The technique for extracting the $t\bar{t}$ cross section from the candidate event sample consists of a binned log likelihood fit of signal and background to the distribution of a discriminant variable in data: the invariant mass of the b-jet and the lepton (M_{lb}). The mass of the three-jet combination with the highest transverse momentum in the event (M3 mass) is used in an alternative approach. The M3 variable is a measure for the hadronic top quark mass, while M_{lb} is related to the leptonic top quark mass. Those two variables provide a good separation between signal and background processes.

This paper is structured as follows: the simulated samples are discussed in Section 2, while Section 3 is dedicated to the event selection. The analysis techniques, including the estimation of the multi-jet background from data, are described in Section 4. The cross-section measurement and the impact of the systematic uncertainties are addressed in Section 5, followed by a summary in Section 6.

2 Data and Simulation

This measurement is performed using 8 TeV proton-proton collisions recorded by the CMS experiment in 2012. A dataset corresponding to an integrated luminosity of up to (2.8 ± 0.1) fb^{-1} is analyzed. Data events are selected by triggers requiring at least one isolated lepton, accompanied by at least three hadronic jets, as discussed in Section 3.

The $t\bar{t}$ selection efficiency is determined with the MADGRAPH [6] Monte Carlo generator, assuming the mass of the top quark to be $m_t = 172.5\,\text{GeV}$. The top quark pairs are generated with up to three additional hard jets, where PYTHIA [7] is used to model parton showering, and the shower matching is done using the Kt-MLM prescription [6]. The $t\bar{t}$ events are normalized to the NLO top quark pair-production cross section $\sigma_{t\bar{t}} = 225.2$ pb calculated using MCFM [2] at

$\sqrt{s} = 8$ TeV for a top quark mass of 172.5 GeV.

Single top quark production is simulated with POWHEG [8, 9]. The W/Z + jets events with leptonic decays of the W/Z vector bosons constitute the largest background. These are also simulated using MADGRAPH with matrix elements corresponding to up to four jets. The W/Z + jets events are generated inclusively with respect to jet flavor. Drell-Yan production of charged leptons is generated for dilepton invariant masses above 50 GeV. In order to benefit from large W + jets samples, W + jets events simulated for 7 TeV are used in this analysis. A PDF-reweighting algorithm is used to correct for the differences between 7 and 8 TeV. Differences in shapes between the two event samples are included in the systematic uncertainties (Section 5).

The background processes are normalized to next-to-leading order (NLO) and next-to next-to-leading order (NNLO) cross-section calculations [2, 10–13], with the exception of QCD multi-jet background, whose normalization is obtained from data (Section 5).

The CMS detector response is simulated using GEANT4 [14] and the simulated events are then processed by the same reconstruction software as the collision data. A detailed description of the CMS detector can be found elsewhere [15].

3 Object Reconstruction and Event Selection

Reconstruction and identification of muons, electrons, photons, neutral and charged hadrons is performed using the particle-flow (PF) algorithm [16]. The energy of electrons is determined from a combination of the track momentum at the primary collision vertex, the corresponding cluster energy in the electromagnetic calorimeter (ECAL), and the energy sum of all bremsstrahlung photons attached to the track. The energy of muons is obtained from the corresponding track momentum using the combined information of the silicon tracker and the muon system [17]. The energy of charged hadrons is determined from a combination of the track momentum and the corresponding energy in the ECAL and in the hadronic calorimeter (HCAL), and calibrated for the non-linear response of the calorimeters. Finally, the energy of neutral hadrons is obtained from the corresponding calibrated ECAL and HCAL energy.

The analysis focuses on the selection of $\mathrm{t\bar{t}}$ semileptonic decays in the electron and in the muon channel, with similar selection requirements applied for the two channels. Candidate $\mathrm{t\bar{t}}$ events are first accepted by one or more dedicated triggers, that require at least one charged lepton, either an electron or a muon, and at least three hadronic jets with transverse momentum $p_T >$ 30 GeV. Triggers requiring at least four hadronic jets (the first two with $p_T > 30$ GeV and the other two with $p_T > 20$ GeV) are employed for part of the data sample. Lepton isolation requirements are applied to improve the purity of the selected sample. Events with a muon in the final state are triggered on presence of a muon candidate with transverse momentum $p_T > 17 - 20$ GeV, depending on the chosen trigger path. Events with an electron candidate are accepted by triggers requiring an electron with $p_T > 25$ GeV.

Signal events are required to have at least one good pp interaction vertex [18] and only one electron or muon, whose origin is consistent with the reconstructed vertex.

Different p_{T} requirements are applied in the offline selections. Muons are required to have a good quality track with $p_{\mathrm{T}} > 26$ GeV and pseudorapidity $|\eta| < 2.1$. Electrons are identified using a combination of the shower shape information and track-electromagnetic cluster matching [19], and required to have $p_{\mathrm{T}} > 30$ GeV and $|\eta| < 2.5$, with the exclusion of the transition region between the barrel and endcap electromagnetic calorimeter, $1.44 < |\eta| < 1.57$. Electrons

coming from photon conversions are vetoed.

Since the lepton from the W boson decay is expected to be isolated from other activity in the event, isolation requirements are applied. We define a relative isolation as $I_{\text{rel}} = (I_{\text{charged}} + I_{\text{photon}} + I_{\text{neutral}})/p_{\text{T}}$, where p_{T} is the transverse momentum of the lepton, and I_{charged}, I_{photon} and I_{neutral} are the sums of the transverse energies of the charged particles, the reconstructed photons, and the neutral particles not identified as photons in a cone of size $\Delta R = \sqrt{\Delta\phi^2 + \Delta\eta^2}$ < 0.3 (0.4 for muons) around the lepton direction, excluding the lepton itself. We require the relative isolation I_{rel} to be less than 0.12 for muons and 0.10 for electrons.

Events with more than one electron or muon candidate with relaxed requirements are vetoed in order to reject Z boson or top-quark-pair decays into dileptons. No explicit requirement is applied on the missing transverse energy.

Jets are clustered from the list of charged and neutral particles reconstructed by the particle flow algorithm [16], using the anti-k_T jet algorithm [20] with a cone size parameter $\Delta R = 0.5$. Particles identified as isolated muons and electrons are not used in the jet clustering. Jet energies are corrected for nonlinearities due to different responses in the endcap and barrel calorimeters, and for the differences between measured and simulated responses [21]. In addition, to account for extra activity from multiple interactions within a jet cone due to additional proton-proton interactions in the same bunch crossing, jet energies are corrected for charged hadrons that belong to a vertex other than the signal primary vertex, and for the amount of pileup expected in the jet area from neutral jet constituents.

At least four jets are required with transverse momenta $p_T > 45$, 45, 35 and 35 GeV, respectively, and $|\eta| < 2.5$. With a trigger requirement of $p_T > 30$ GeV, the $p_T > 45$ GeV threshold value ensures to be in the trigger efficiency plateau region.

To reduce contamination from background processes, at least one of the jets has to be identified as a b-jet. The Jet Probability [22] algorithm is used, where the discriminator is defined as the probability that all tracks with positive impact parameter come from the primary vertex. Figure 1 shows the M_{lb} distribution after applying a b-tag algorithm. The M_{lb} analysis uses the data-driven method described in [22] for the estimation of the b-tagging efficiency. B-tagging is applied on the jet assigned to the leptonically decaying top quark.

In the M3 analysis similar requirements for the selection of $\mathrm{t\bar{t}}$ semileptonic decays were used, with slightly different p_{T}-threshold values. Only the differences with respect to the main selection are summarized in the following.

Events in the muon channel are triggered on presence of an isolated muon candidate with transverse momentum $p_T > 24$ GeV and at least three hadronic jets with $p_T > 30$ GeV. Electrons are selected in the barrel ($|\eta| < 1.44$) of the electromagnetic calorimeter. At least four jets are required with transverse momenta $p_T > 45$, 45, 45 and 20 GeV, and $|\eta| < 2.5$. The electron selection applies a p_{T}-dependent turn-on scale factor on the fourth jet.

The M3 analysis uses a scale factor of (0.97 ± 0.06) [23] to the simulated events to take into account the different b-tagging efficiency and the different probability that a light quark or a gluon jet is identified as a b-jet in data and simulation.

4 Analysis strategy and techniques

The number of signal events is determined with a binned maximum likelihood fit of templates describing signal and background processes to the data sample passing the final selection, by

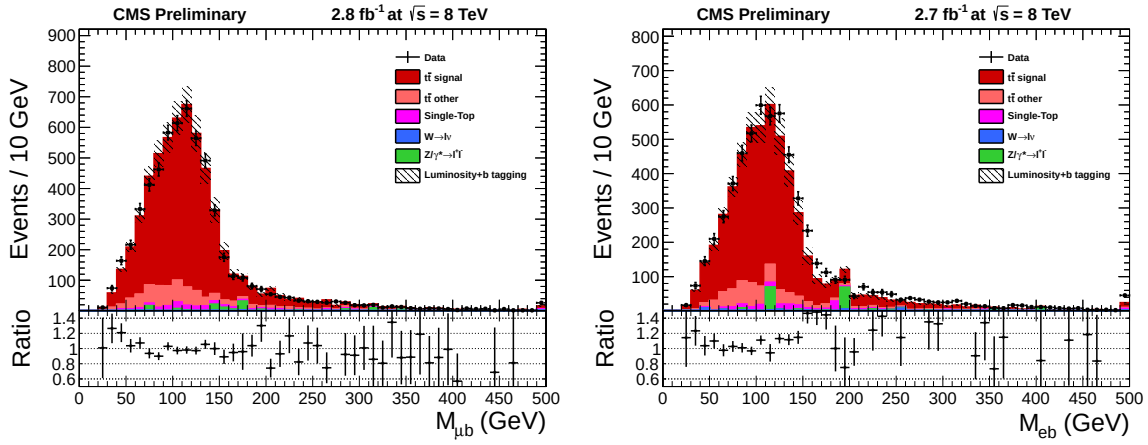

Figure 1: Distribution of the jet-lepton mass for all relevant processes in the muon + jets channel (left) and the electron + jets channel (right), after applying a b-tag. The data correspond to an integrated luminosity of 2.8 fb^{-1} for the muon channel and 2.7 fb^{-1} for the electron channel. The multi-jet background is not shown. The plots are already corrected for the b-tagging efficiency scale factor. The uncertainty bands include the uncertainty on the luminosity measurement and the b-tagging systematic uncertainty. The ratio between data and simulation is shown in the lower panels.

fitting M_{lb}, the invariant mass distribution of the b-jet and the lepton. M_{lb} is related to the the leptonic top quark mass and provides a good separation between signal and background processes.

The $\text{t}\bar{\text{t}}$, single-top, W + jets, and Z + jets templates, used in the likelihood maximization, are taken from simulation, while the QCD template is estimated from data, using the anti relative isolation technique described in Section 4.1.

The template fit is performed after b-tagging. One single template is used for $\text{t}\bar{\text{t}}$ events (both for the $\text{t}\bar{\text{t}}$ signal events and the other $\text{t}\bar{\text{t}}$ events passing the selection criteria) and one single template for all background processes, except the multi-jet one, whose normalization is determined by the fit itself.

4.1 Estimation of the multi-jet background from data

Monte-Carlo simulation can not adequately reproduce the shape and size of the QCD multi-jet background. This background is estimated from data. Selected multi-jet events are mostly comprised of semi-leptonic heavy-flavour decays and, in the electron channel, events in which pion-rich jets fake electrons. We take advantage of the fact that such events feature lepton candidates not coming from W boson decay and thus not truly isolated. We therefore extract the shape of the accepted multi-jet background from a side-band data sample specially selected such that it is rich in background and poor in signal. For this purpose we require leptons with large relative isolation, greater than 0.25 in the electron channel and 0.17 in the muon channel. These values are chosen so as to balance number of events and contamination of the sideband data by signal events and events originating from other background processes such as W + jets. Biases from these sources are minimized by removing the remaining $\text{t}\bar{\text{t}}$, W + jets and Z + jets contamination using simulation. Other backgrounds, for example single top, are neglected. The nominal multi-jet shape is taken as the distribution measured in the sideband after subtracting the components described above.

5 Cross Section Measurement

The $t\bar{t}$ production cross section is extracted from the number of $t\bar{t}$ events observed in the data, using the equation:

$$\sigma_{t\bar{t}} = \frac{N_{t\bar{t}}}{L \cdot \varepsilon_{t\bar{t}} \cdot BR}. \quad (1)$$

$N_{t\bar{t}}$ is the number of $t\bar{t}$ events, L is the integrated luminosity, $\varepsilon_{t\bar{t}}$ is the efficiency for signal events to pass the selection requirements for the specific channel, and BR is the branching ratio of the channel considered. The number of signal events is determined with a template fit as discussed in Section 4.

Figure 2 shows the result for the fit to the data distributions. A simultaneous fit to the M_{lb} data distribution in the electron and muon channels is performed to obtain the combined result. Separate fit parameters are used to scale the normalized QCD templates in the two channels.

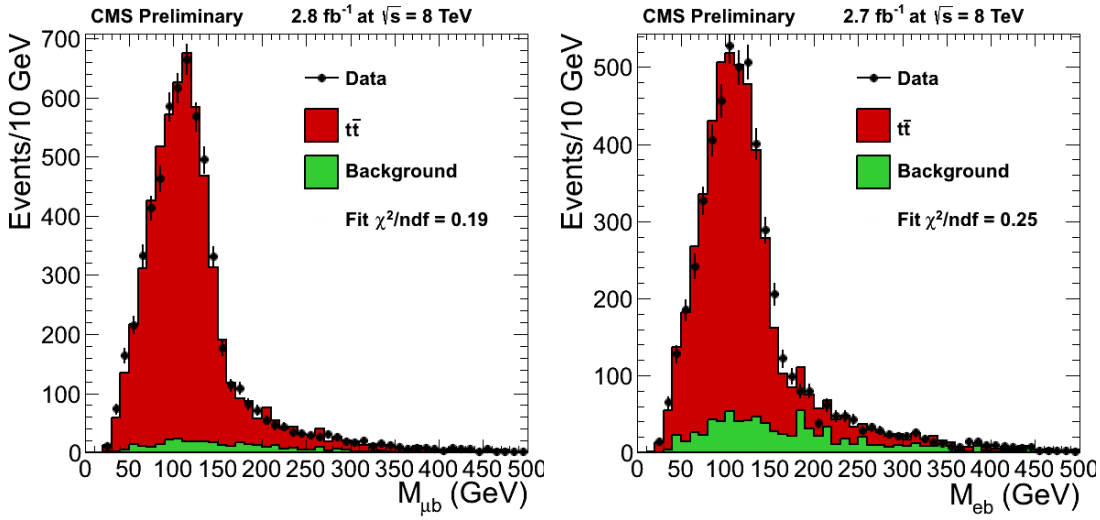

Figure 2: Template fit result on the lepton-jet mass in the muon + jets (left) and in the electron + jets channel (right). The data corresponds to an integrated luminosity of 2.8 fb^{-1} in the muon channel and 2.7 fb^{-1} in the electron channel. B-tagging is applied. Signal and background contributions are rescaled according to the fit results.

We determine a signal selection efficiency times branching fraction $\varepsilon_{t\bar{t}} \cdot BR$ of 3.2% in the muon channel and 2.9% in the electron channel, as shown in Table 1. Trigger efficiency scale factors of 98.6% for the electron channel and 98.1% for the muon channel, flat in p_T, have been determined from data-Monte Carlo comparison and are applied to the simulation to improve the description of the data in the trigger efficiency and lepton identification criteria.

The measured cross section with the lepton-jet mass template fit is:

$$\sigma_{t\bar{t}}(\mu + jets) = 229.9 \pm 11.1\ (\text{stat.})^{+27.6}_{-29.0}\ (\text{syst.}) \pm 10.1\ (\text{lum.})\ \text{pb},$$
$$\sigma_{t\bar{t}}(e + jets) = 227.3 \pm 12.2\ (\text{stat.})^{+35.5}_{-30.0}\ (\text{syst.}) \pm 10.0\ (\text{lum.})\ \text{pb},$$
$$\sigma_{t\bar{t}}(combined) = 228.4 \pm 9.0\ (\text{stat.})^{+29.0}_{-26.0}\ (\text{syst.}) \pm 10.0\ (\text{lum.})\ \text{pb},$$

where the systematic uncertainties are discussed in the next Section 5.1.

Table 1: Signal selection efficiencies, determined from simulation. The $t\bar{t}$ selection efficiency $\varepsilon_{t\bar{t}} \cdot BR$, is the number of selected $t\bar{t}$ events out of all produced $t\bar{t}$ pairs, in all decay channels. The signal efficiency, $\varepsilon_{t\bar{t}}$, is the number of selected signal events specific to the decay channel being studied, out of the produced signal events in the decay channel under study.

Channel	$t\bar{t}$ selection efficiency ($\varepsilon_{t\bar{t}} \cdot BR$)	signal efficiency ($\varepsilon_{t\bar{t}}$)
Electron	2.9%	15.1%
Muon	3.2%	24.0%

5.1 Systematic uncertainties

Several contributions to the systematic uncertainty are considered and their effects are determined by propagating them to the cross-section measurement, in the electron channel, in the muon channel and in the combined measurement. Template shapes and signal efficiencies are varied together according to the systematic uncertainty considered. The uncertainty is determined on data as the variation of the cross section and it is cross-checked with pseudoexperiments.

Most systematic uncertainties are common to both measurements. The effect of the jet energy scale (JES) and jet energy resolution (JER) are evaluated by varying them up and down within the p_T- and η-dependent uncertainties [24]. The uncertainty related to the pile-up modeling is determined by propagating a $\pm 5\%$ variation to the central value of the minimum-bias cross section. Variations in the composition of the main background processes, W + jets and Z + jets, are evaluated by varying each of them by $\pm 50\%$. The systematic uncertainty due to the PDF-reweighting procedure has been estimated by using the 8 TeV W + jet samples to produce the varied templates and by comparing to the PDF-reweighted 7 TeV samples.

The b-tagging efficiency for b-jets is measured using a data-driven technique described in [22] on the same selected event sample as that for the cross-section determination but before b-tagging. Taking into account the correlation between the cross-section estimator and the b-tagging efficiency estimator, the statistical uncertainty on the estimated b-tagging efficiency obtained on the 8 TeV data sample is propagated into the statistical uncertainty of the cross-section measurement. The systematic uncertainty on the estimated b-tagging efficiency on the other hand is propagated into the systematic uncertainty of the cross-section measurement. The systematic uncertainty quoted in [22] is conservatively multiplied by a factor of 1.5 when propagating it from 7 TeV to 8 TeV. The mistag rate uncertainties on c- and light-quarks as quoted in [22] are also multiplied by a factor of 1.5 and propagated as well into the systematic uncertainty of the cross-section measurement. The propagation of the uncertainties takes into account the relative fractions of quark flavours, as obtained from simulation, of the b-tagged jet connected to the leptonic decaying top quark.

Theoretical uncertainties are taken from detailed studies performed on 7 TeV MC samples. They include the factorization scale, where a variation of a factor 0.5 and 2 is applied to the $t\bar{t}$ and W + jet Q^2-scale. The effect of the jet-parton matching threshold on $t\bar{t}$ and W + jets events is studied by varying the threshold used for matching the matrix element level to the particles created in the parton showering by a factor of 0.5 or 2. PDF uncertainties are evaluated by varying up and down the parameters of the CTEQ6.6 PDF set. The uncertainty due to the top quark mass is evaluated by varying the top quark mass by ± 1.5 GeV [25] corresponding to the accuracy of the world average measurement.

An uncertainty of 4.4% [26] is assigned to the knowledge of the luminosity.

Table 2 provides an overview of the contributions to the systematic uncertainty on the combined cross-section measurement.

Table 2: Overview of the systematic uncertainties (in %) on the cross-section measurement. Uncertainties marked with (*) are obtained from 7 TeV. The luminosity uncertainty of 4.4% is not included in the total.

Systematic	Combined fit $\delta\sigma_{t\bar{t}}$ (%)	
Jet Energy Scale	+4.3	-5.0
Jet Energy Resolution	+0.5	-1.1
Pileup	+0.7	-0.7
Background Composition	+0.1	-0.1
W + Jets template shape from unweighted 7 TeV	+0.9	-0.9
Normalisation of data-driven multijet shape	+0.9	-0.9
b tagging efficiency measurement	+8.0	-8.0
Trigger Efficiency	+3.2	-2.8
Lepton selection	+2.8	-2.4
Factorization scale (*)	+6.2	-2.1
ME-PS Matching threshold (*)	+4.6	-3.1
PDF uncertainties (*)	+1.6	-2.0
Top Quark Mass (*)	+0.3	-1.4
Total	+12.7	-11.4
Luminosity	+4.4	-4.4

5.2 Alternative approach using M3

The M3 distributions in the electron and muon channel are shown in Figure 3. Good agreement is observed between data and the templates. Results are compatible with the M_{lb} analysis.

6 Summary

We performed a measurement of the $t\bar{t}$ production cross section at $\sqrt{s} = 8\,\text{TeV}$, using the data collected with the CMS detector corresponding to an integrated luminosity of up to 2.8 fb^{-1}.

The $t\bar{t}$ cross section is extracted using a binned maximum likelihood fit of templates from simulated events to the data sample. From the combined analysis of the electron + jets and the muon + jets channels we obtain a result of:

$$\sigma_{t\bar{t}} = 228.4 \pm 9.0\,(\text{stat.})^{+29.0}_{-26.0}\,(\text{syst.}) \pm 10.0\,(\text{lum.})\,\text{pb},$$

in agreement with QCD predictions, based on the full NLO matrix elements and approximate NNLO calculations, which provide: $\sigma_{t\bar{t}} = 202.5^{+11.3}_{-14.5} \pm 8.5$ pb (for ABM11 PDFs) [27], $\sigma_{t\bar{t}} = 249.9^{+14.0}_{-18.2}\,{}^{+6.2}_{-6.3}$ pb (for MSTW PDFs) [27], $\sigma_{t\bar{t}} = 228.6^{+18.2}_{-19.8}\,{}^{+5.6}_{-5.9}$ pb [28], $\sigma_{t\bar{t}} = 234^{+10}_{-7} \pm 12$ pb [29], $\sigma_{t\bar{t}} = 224.7^{+11.8}_{-12.2}\,{}^{+10.8}_{-11.6}$ pb [30], where the first uncertainty is from scale variation and the second from PDF.

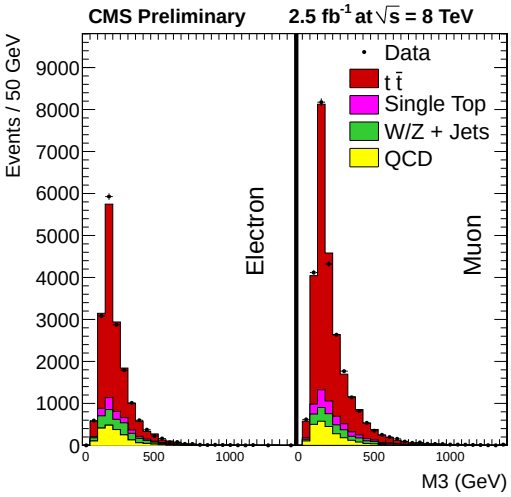

Figure 3: Result of the M3 template likelihood fit to 2012 data for the combined channel. B-tagging is applied. Signal and background contributions are rescaled according to the template fit results. The data correspond to an integrated luminosity of 2.3 fb^{-1} in the electron channel and 2.7 fb^{-1} in the muon channel.

The measured cross section agrees with the one obtained from final states with two leptons. The combination of the two measurements and its comparison with theoretical predictions are presented in [31].

References

[1] L. Evans and P. Bryant (editors), "LHC Machine", *JINST* **3** (2008) S08001, doi:10.1088/1748-0221/3/08/S08001.

[2] J. Campbell and R. Ellis, "MCFM for the Tevatron and the LHC", *FERMILAB-Conf-10-244-T* (2010) 205–206, arXiv:hep-ph/1007.3492.

[3] CMS Collaboration, "Measurement of the $\text{t}\bar{\text{t}}$ production cross section in pp collisions at 7 TeV the lepton+jets events using b-quark jet identification", *Phys. Rev.* **D 84** (2011) 092004, doi:10.1103/PhysRevD.84.092004, arXiv:1108.3773.

[4] CMS Collaboration, "Top pair cross section in e/mu + jets", *CMS Physics Analysis Summary* **CMS-PAS-TOP-11-003** (2011).

[5] ATLAS Collaboration, " Measurement of the top quark pair production cross section with ATLAS in the single lepton channel", arXiv:1201.1889. Submitted to Phys. Lett. B.

[6] J. Alwall et al., "MadGraph/MadEvent v4: The New Web Generation", *JHEP* **09** (2007) 028, doi:10.1088/1126-6708/2007/09/028, arXiv:0706.2334.

[7] T. Sjostrand, S. Mrenna, and P. Z. Skands, "PYTHIA 6.4 Physics and Manual", *JHEP* **05** (2006) 026, doi:10.1088/1126-6708/2006/05/026, arXiv:hep-ph/0603175.

[8] S. Alioli, P. Nason, C. Oleari et al., "NLO Vector-Boson Production Matched with Shower in POWHEG", *JHEP* **07** (2008) 060, doi:10.1088/1126-6708/2008/07/060.

[9] S. Frixione, P. Nason, and C. Oleari, "Matching NLO QCD Computations with Parton Shower simulations: the POWHEG method", *JHEP* **11** (2007) 070, doi:10.1088/1126-6708/2007/11/070.

[10] R. Gavin, Y. Li, F. Petriello et al., "FEWZ 2.0: A code for hadronic Z production at next-to-next-to-leading order", *Comp. Phys. Commun.* **182** (2011) 2388, doi:10.1016/j.cpc.2011.06.008, arXiv::1011.3540v1.

[11] R. Gavin, Y. Li, F. Petriello et al., "W physics at the LHC with FEWZ 2.1", (2012) arXiv:1201.5896v1.

[12] J. M. Campbell and F. Tramontano, "Next-to-leading order corrections to W t production and decay", *Nucl. Phys.* **B 726** (2005) 109–130, doi:10.1016/j.nuclphysb.2005.08.015, arXiv:hep-ph/0506289.

[13] J. M. Campbell, R. K. Ellis, and F. Tramontano, "Single top production and decay at next-to-leading order", *Phys. Rev.* **D 70** (2004) 094012, doi:10.1103/PhysRevD.70.094012, arXiv:hep-ph/0408158.

[14] J. Allison et al., "Geant4 developments and applications", *IEEE Trans. Nucl. Sci.* **53** (2006) 270, doi:10.1109/TNS.2006.869826.

[15] CMS Collaboration, "The CMS experiment at the CERN LHC", *JINST* **0803** (2008) S08004, doi:10.1088/1748-0221/3/08/S08004.

[16] CMS Collaboration, "Commissioning of the Particle-Flow Reconstruction in Minimum-Bias and Jet Events from pp Collisions at 7 TeV", *CMS Physics Analysis Summary* **CMS-PAS-PFT-10-002** (2010).

[17] CMS Collaboration, "Performance of muon identification in pp collisions at $\sqrt{s}$ = 7 TeV", *CMS Physics Analysis Summary* **CMS-PAS-MUO-10-002** (2010).

[18] CMS Collaboration, "CMS Tracking Performance Results from Early LHC Operation", *CMS Physics Analysis Summary* **CMS-PAS-TRK-10-001** (2010) arXiv:1007.1988.

[19] CMS Collaboration, "Electron reconstruction and identification at $\sqrt{s}$=7 TeV", *CMS Physics Analysis Summary* **CMS-PAS-EGM-10-004** (2010).

[20] M. Cacciari, G. P. Salam, and G. Soyez, "The anti-kt jet clustering algorithm", *JHEP* **04** (2008) 063, arXiv:0802.1189.

[21] CMS Collaboration, "Determination of Jet Energy Calibration and Transverse Momentum Resolution in CMS", arXiv:1107.4277. Submitted to JHEP.

[22] CMS Collaboration, "Measurement of b-tagging efficiency using ttbar events", *CMS Physics Analysis Summary* **CMS-PAS-BTV-11-003** (2011).

[23] CMS Collaboration, "b-jet identification in the CMS Experiment", *CMS Physics Analysis Summary* **CMS-PAS-BTV-11-004** (2012).

[24] CMS Collaboration, "Jet Energy Calibration and Transverse Momentum Resolution in CMS", *CMS Physics Analysis Summary* **CMS-PAS-JME-10-011** (2011).

[25] J. Beringer et al., "(Particle Data Group)", *Phys. Rev.* **D 86** (2012) 010001.

[26] CMS Collaboration, "CMS Luminosity Based on Pixel Cluster Counting - Summer 2012 Update", *CMS Physics Analysis Summary* **CMS-PAS-LUM-12-001** (2012).

[27] S. Moch, P. Uwer, and A. Vogt, "On top-pair hadro-production at next-to-next-to-leading order", (2012) arXiv:1203.6282.

[28] M. Cacciari, M. Czakon, M. L. Mangano et al., "Top-pair production at hadron colliders with next-to-next-to-leading logarithmic soft-gluon resummation", (2011) arXiv:1111.5869.

[29] N. Kidonakis, "Differential and total cross sections for top pair and single top production", (2012) arXiv:1205.3453.

[30] V. Ahrens, A. Ferroglia, M. Neubert et al., "Precision predictions for the $t\bar{t}$ production cross section at hadron colliders", (2011) arXiv:1105.5824.

[31] CMS Collaboration, "Measurement of the ttbar production cross section in the dilepton channel in pp collisions at $\sqrt{s} = 8$ TeV", *CMS Physics Analysis Summary* **CMS-PAS-TOP-12-007** (2012).